International Journal of Engineering Science 192 (2023) 103928

Contents lists available at ScienceDirect

International Journal of Engineering Science

journal homepage: www.elsevier.com/locate/ijengsci

An asymptotic approach for large amplitude motions of generic nonlinear systems

Stefano Lenci

Department of Civil and Building Engineering and Architecture, Polytechnic University of Marche, 60131 Ancona, Italy

ARTICLE INFO

Keywords:
Asymptotic methods
Large amplitude oscillations
Duffing equation
Near peak exact behavior

ABSTRACT

Starting from the observation that classical asymptotic methods fail to correctly describe the resonance peak of the frequency response curve of a nonlinear oscillator under moderate and large excitation amplitudes, an alternative approach is proposed to overcome this problem. The differences between the multiple time scale method (one of the most performant classical methods) and numerical simulations are initially shown with reference to on the paradigmatic Duffing equation. They are also shown some characteristics of the near peak behavior. Then, the proposed asymptotic approach is illustrated. The basic idea is that of having the zero-order problem nonlinear, while in classical methods it is linear. Thanks to the energy conservation, the zero-order problem is solved exactly. Also, the exact solution of the higher-order problems is obtained in closed-form, thus providing a fully analytical approach. Although the proposed method is valid for any kind of motion, special attention is dedicated to periodic nonlinear oscillations, because of their interest in practical applications. A simple formula for determining the *exact* intersection of the frequency response and backbone curves is obtained, and it is shown that it can be computed without the need of solving explicitly not even the zero-order problem. Some illustrative examples are finally reported.

1. Introduction

Many mathematical techniques have been developed in the past to obtain approximate analytical solutions of problems for which close form expressions are not available: complex variable, matched asymptotic expansion boundary layer, multiscale asymptotic homogenization (Bensoussan, Lions, & Papanicolaou, 2011; Yang, Sun, Liu, & Cui, 2021) (for static problems), Wentzel, Kramers and Brillouin (WKB), Krylov, Bogoliubov and Mitropolski (KBM), homotopy, Poincaré–Lindstedt, slowing varying frequency, multiple time scale method (for dynamic problems), etc. Although in a different way and with different approaches, they (i) are somehow based on the use of a small parameter ε (naturally present in the problem or artificially introduced), (ii) are reliable when this parameter is small, and thus (iii) are named *asymptotic development* or *perturbations* methods. A detailed description of all of them is not possible, and it is out of the scope of this work. Thus, we refer to classical textbooks (Awrejcewicz, Andrianov, & Manevitch, 1998; Awrejcewicz & Krysko, 2006; Bogoliubov & A., 1961; Hinch, 1991; Holmes, 1995; Kevorkian & Cole, 1981; Nayfeh, 1973, 1993; Nayfeh & Mook, 1995; Rand & Armbruster, 1987) for better insight, including the differences between each other, required tricks, potentialities, and limits of use.

Asymptotic methods are commonly used in nonlinear dynamics, in particular in mechanics of structures, like for example in portal frames (Brasil, 1999), gear systems (Nie, Zheng, Yu, Wen, & Dai, 2013), externally excited NES-controlled systems (Luongo & Zulli, 2012), rotating pendulum (Xu & Wiercigroch, 2007), internal resonances (Clementi, Lenci, & Rega, 2020), nonlinear vibration of uniform beams (Atluri, 1973) and cables (Guo, Rega, Kang, & Wang, 2020; Srinil & Rega, 2007), non-uniform cables and

E-mail address: lenci@univpm.it.

https://doi.org/10.1016/j.ijengsci.2023.103928
Received 6 November 2022; Received in revised form 26 May 2023; Accepted 9 July 2023
Available online 23 July 2023

beams (Lenci, Clementi, & Mazzilli, 2013), nonlocal strain gradient beams (Li & Hu, 2016), inclined risers (Alfosail & Younis, 2020), galloping problems (Luongo, Zulli, & Piccardo, 2008), wave propagation in metamaterials (Fortunati, Bacigalupo, Lepidi, Arena, & Lacarbonara, 2022), electrostatically actuated resonators (Ilyas, Alfosail, & Younis, 2019), shells (Gonçalves, Silva, & Del Prado, 2008), Atomic Force Microscopy (Settimi, Gottlieb, & Rega, 2015), bifurcation problems (Luongo, 2017), control (Bauomy & Taha, 2021). This list is far from exhaustive, and the frontier is to apply asymptotic methods directly to partial differential equations, without an a priori reduced order model (Kloda, Lenci, Warminski, & Szmit, 2022). Although mechanical engineering is the natural background of the present work (Cartmell, Ziegler, Khanin, & Forehand, 2003), it is worth underlining that these techniques, and the herein proposed development, are general and in principle can be applied to a much larger class of problems.

The common feature consists of a Taylor expansion with respect to ε of the solution, and then of the equations of the problem, thus obtaining a sequence of problems to be solved one after the other up to the desired order. The larger the required precision, the larger the number of problems to be solved, and the more the requested computational effort. It is commonly accepted that a method is satisfactory only if it provides good enough results by solving few problems only (Nayfeh, 1973).

Another commonly accepted cornerstone is that all the sequential problems ensuing from the Taylor expansion are *linear*, in particular the lowest one, which is the most important. This is clearly due to the easiness of obtaining the closed-form solutions for linear problems, in agreement with the goal of these approaches which is to have *analytical* – although approximate – expressions for the solution. This is commonly obtained in two different ways:

1. having that the lowest-order term of the solution is proportional to ε (Kloda, Lenci, & Warminski, 2018). This entails that the solution is valid only for moderately large amplitudes;
2. assuming that all nonlinear terms are small (i.e. proportional to ε) (Razzak, Alam, & Sharif, 2018; Ren, Yao, & He, 2019). The disadvantage of this latter approach is that it does not provide reliable results for strongly nonlinear systems.

These drawbacks are better illustrated, also from a quantitative point of view, in Section 2.

Based on the previous motivation, and to obtain an asymptotic method that gives reliable solutions for large amplitudes and strongly nonlinear systems, an original approach is proposed in this work. It consists of having a lowest-order problem that is *nonlinear*, while the higher-order problems are linear. As we will see later on, there is a class of nonlinear problems for which the solutions can be obtained analytically, and thus we are not giving up the possibility to have closed-form solutions while extending them to a wider class of problems and cases.

There have been some developments in the literature that may appear similar to a first glance, but they are not.

In Hsu (1960) the author does not consider damping and, more important, considers an excitation that is an elliptic function (Section 3; note that this implies that the excitation varies with the oscillation amplitude, and is not fixed). In Section 4 he considered the case of harmonic excitation, still with damping. Initially, he proposed an error function and approximate the solution by means of an elliptic function. Then, he considered the first harmonic of the Fourier series obtained in Section 3 to find an approximate relation between the excitation amplitude and the solution amplitude; he then proposed various developments considering higher order terms in the Fourier expansion of the Elliptic functions, ending with an approximate solution (his Eq. (50)) that is substantially equivalent to that obtained by the harmonic balance method. Thus, the approach is completely different with respect to that used in this work. In addition to the methodological difference illustrated above, in Hsu (1960) there is no damping, and so no peak of the frequency response curve, where instead the present analysis is focused.

In Elias-Zuniga (2005) the author considers the Duffing equation where the excitation is an elliptic function as in Hsu (1960), but adds the damping term (which is the element of novelty). As in Hsu (1960), the exact solution is sought as the combination of elliptic functions, leading to a strongly nonlinear equation (his Eq. (7)) that cannot be solved in close form. Thus, the elliptic function is approximated by its Fourier series, limited to the first harmonic, and the author proceeds with the harmonic balance method. Again, this approach is completely different with respect to that used in this work. In Elias-Zuniga (2006) the same method is applied, with very minor changes. In subsequent works, the author applied his method, which he named the Elliptic Balance Method, to systems with more degrees of freedom.

In Belhaq and Lakrad (2000) the authors introduced the slow time scales. One of the results of the present work is to show that it is possible to have relevant information (near the peak) without using the multiple time scale method, entailing a much easier mathematical development. Furthermore, the authors do not illustrate the solution, but show only the analytical developments. We mention (Chen & Cheung, 1997) (that somehow inspired (Belhaq & Lakrad, 2000)) where the same approach is used, too, but introducing the asymptotic expansion of the frequency, according to the Lindstedt–Poincaré method. Again, the difference with respect to the present work is that we obtain important information without the necessity to expand the frequency. On top of the previous comments, the major difference between these two papers and the present work is that they do *not* consider external excitation, and thus deal with a different problem (and accordingly they do not report frequency response curves).

Section 4 of Kovacic, Cveticanin, Zukovic, and Rakaric (2016) deals with autonomous systems, i.e. no excitation, and so the previous considerations apply. In Section 5, on the other hand, the forced case is considered. Here the authors summarize – with some minor differences – the results of Elias-Zuniga (2005), Hsu (1960) (according to the Review nature of Kovacic et al. (2016)), and thus the previous comments apply. To further underline the difference, we note that when dealing with harmonic excitation (the case of interest here), see Section 5.2 of Kovacic et al. (2016), other papers are quoted, but they used the method of averaging or energy conservation law, which are completely different from the proposed approach.

The previous works are valid only for the Duffing equation, while the proposed approach can be applied to any nonlinear system, and thus is much more general and extensive.

This paper is organized as follows. In Section 2 the main limitations of the classical asymptotic problems are illustrated in detail, also highlighting some properties that are not well known, at least to the best of the author's knowledge. Then, in Section 3 the proposed approach is illustrated and then applied for illustrative purposes to various systems (Section 4), among which the most detailed is the Duffing oscillator (Section 4.2), also because of the importance of this prototype equations. The paper ends with some conclusions and suggestions for further developments (Section 5).

2. Limits of the classical asymptotic development methods

Although the proposed idea (Section 3) is of general validity, and can be applied to many nonlinear systems, for the sake of concreteness it is useful to illustrate the drawbacks of classical asymptotic methods (here) and the suggested improvements (Section 4.2) with reference to a specific example. We choose the Duffing equation (Duffing, 1918)

$$\hat{m}\ddot{\hat{x}} + \hat{\delta}\dot{\hat{x}} + \hat{k}_1\hat{x} + \hat{k}_3\hat{x}^3 = \hat{F}\cos(\hat{\omega}\hat{t}) \tag{1}$$

because it is an archetypal nonlinear oscillator, that has been largely investigated in the literature (Brennan & Kovacic, 2011). It founds applications in many problems (Parzygnat & Pao, 1978), and thus it has also an interest *per se*, not only as an illustrative case.

In this work, we are mainly interested in the case in which there are nonlinear oscillations around the undamped unforced rest position $\hat{x} = 0$. Thus, we assume $\hat{k}_1 > 0$. We also assume $\hat{k}_3 > 0$, even if this hypothesis can be relaxed without problems, and also the softening case $\hat{k}_3 < 0$ can be considered similarly. With these assumptions, by setting

$$\hat{x} = x\frac{\sqrt{\hat{k}_1}}{\sqrt{\hat{k}_3}}, \quad \hat{t} = t\frac{\sqrt{\hat{m}}}{\sqrt{\hat{k}_1}}, \quad \hat{\delta} = \delta\sqrt{\hat{m}}\sqrt{\hat{k}_1}, \quad \hat{F} = F\frac{\hat{k}_1^{3/2}}{\sqrt{\hat{k}_3}}, \quad \hat{\omega} = \omega\frac{\sqrt{\hat{k}_1}}{\sqrt{\hat{m}}}, \tag{2}$$

Eq. (1) can be rewritten, without loss of generality, in the dimensionless and simpler form

$$\ddot{x} + \delta\dot{x} + x + x^3 = F\cos(\omega t), \tag{3}$$

that will be considered in the following. Note that for (3) the natural linear frequency is $\omega_0 = 1$.

The two approaches mentioned in the introduction are the following:

1. $\ddot{x} + \varepsilon\delta\dot{x} + x + x^3 = \varepsilon^2 F\cos(\omega t)$ and $x(t) = \varepsilon x_0(t) + \varepsilon^2 x_1(t) + \varepsilon^3 x_2(t) + \cdots$;
2. $\ddot{x} + \varepsilon\delta\dot{x} + x + \varepsilon x^3 = \varepsilon F\cos(\omega t)$ and $x(t) = x_0(t) + \varepsilon x_1(t) + \varepsilon^2 x_2(t) + \cdots$.

Both lead to the same *linear* lowest-order problem

$$\ddot{x}_0 + x_0 = 0, \tag{4}$$

which is the leading one.

By applying the classical Multiple Times Scale asymptotic Method (MTSM) (Nayfeh & Mook, 1995) the solution is given by, up to the first-order,

$$x = A\cos(\omega t + \psi) + \cdots, \tag{5}$$

where the relation between the frequency and the amplitude is

$$\omega_{nl} = 1 + \frac{3}{8}A^2 + \cdots, \tag{6}$$

$$\omega = \omega_{nl} \pm \sqrt{\left(\frac{F}{2A}\right)^2 - \left(\frac{\delta}{2}\right)^2}. \tag{7}$$

The first one gives the so-called Backbone Curve (BC), i.e. the relation between the amplitude and the frequency of the solution in the undamped unforced case, the latter the Frequency Response Curve (FRC), i.e. the same relation but now considering damping and excitation.

To show the limits of the classical asymptotic approach, we now compare (6) and (7) with the non-asymptotic solution of the Duffing equation. Now $A = x_{\max} = \max_{t\in[0,T]} x(t) = -\min_{t\in[0,T]} x(t)$, which is the same of (5) in the limit of small amplitudes.

For the backbone curve the *exact* expression is reported in the forthcoming Eq. (52), where we identify $x_{\max}$ with its first-order approximation A. The non-asymptotic FRCs are obtained by numerical integrations of (3) since their exact expressions are not available. We fix $\delta = 0.05$ and vary F and ω.

The comparison for low values of F is reported in Fig. 1. From Fig. 1a we see a very good agreement between classical asymptotic and non-asymptotic results, both for the backbone as well as for the FRCs. In Fig. 1b it is also reported the (numerical) phase difference between the excitation and the solution, i.e. the time delay between the maximum of the solution and the maximum of the excitation. It must be underlined that in correspondence with the resonance the phase difference is around 1/4 of the period, which agrees with the well-known results of the linear case. This is because the excitation amplitude is small and thus we are yet almost in the linear regime, even if the hardening behavior of the backbone curves is already visible in Fig. 1a.

Although at the full scale of Fig. 1a there is a good agreement, as said above, if we zoom around the peak of the FRC we note some differences (Fig. 1c), of the order of 3%. They are compatible with the approximate nature of the analytical solution, even if

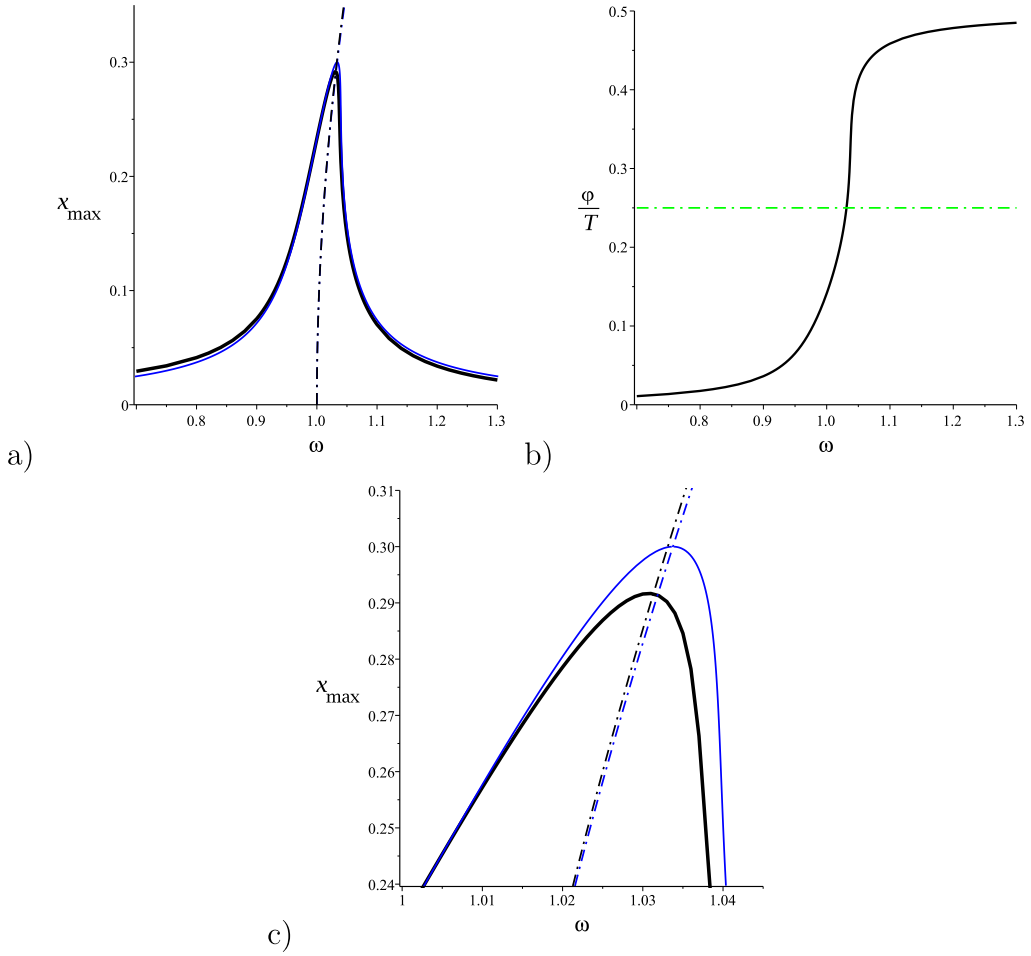

Fig. 1. (a) The backbone (dash–dot) and frequency response (continuous) curves for $\delta = 0.05$ and $F = 0.015$. Blue curves are the asymptotic solutions, and black curves are the exact/numerical ones. (b) The phase difference between the excitation and the solution (only for the numerical solution). (c) Zoom of the case (a) around the peak.

they are around the most critical point (where the displacement is maximum), and thus reveal an unpleasant characteristic of the classical asymptotic solution: the error is maximum where more care is needed.

By increasing the excitation amplitude F up to "medium" values, the difference becomes more important, as shown in Fig. 2a. In this case a better approximation can likely be obtained by going up to the next order in the classical asymptotic development, even if this is somehow in contrast with the "philosophy" of the method, that suggests using only few terms in the asymptotic development.

For "large" values of F the difference becomes huge (Fig. 3a), and by no means the classical asymptotic solution can be used to approximate the true solution, even using higher-order terms in the expansion.

By increasing F, the phase of the solution has a turning point around $1/4$ of the period, as shown in Figs. 2b and 3b.

The conclusion is that asymptotic methods can be used only for small values of the forcing, and even in this case they introduce errors where more care is needed (close to the peak of the FRCs). Although the previous results are obtained only with the MTSN, they hold also for different versions of classical asymptotic methods.

The reason behind the bad approximation for large excitation amplitude relies on the fact that the first-order problem (4), which is the dominating ones, is linear. Since higher-order terms provide small correction to the first-order one (being ϵ small), we cannot expect to have a good approximation far from the linear case. Since in the linear case the backbone curve is vertical (the frequency does not depend on the amplitude in the free dynamics case), asymptotic methods are expected to give good approximations only when the exact solution (i.e. the FRC) is in its neighborhood, i.e. in the light gray region schematically illustrated in Fig. 4. This is further and indirectly confirmed by the fact that in Eq. (1)a the error becomes visible for values of ω far from the resonant frequency $\omega = 1$, even if this is not relevant for our purposes.

The previous considerations suggest how to improve the classical methods, still remaining in an asymptotic framework: try to develop around the exact, bent, backbone curve (or at least around its *nonlinear* approximation), not around the linear one. In other

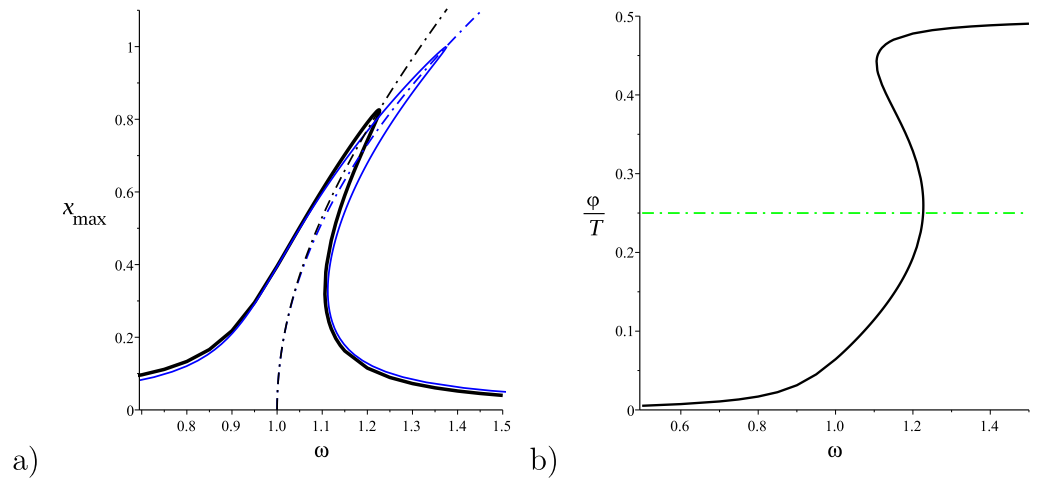

Fig. 2. (a) The backbone (dash–dot) and frequency response (continuous) curves for $\delta = 0.05$ and $F = 0.05$. Blue curves are the asymptotic solutions, and black curves are the exact/numerical ones. (b) The phase difference between the excitation and the solution (only for the numerical solution).

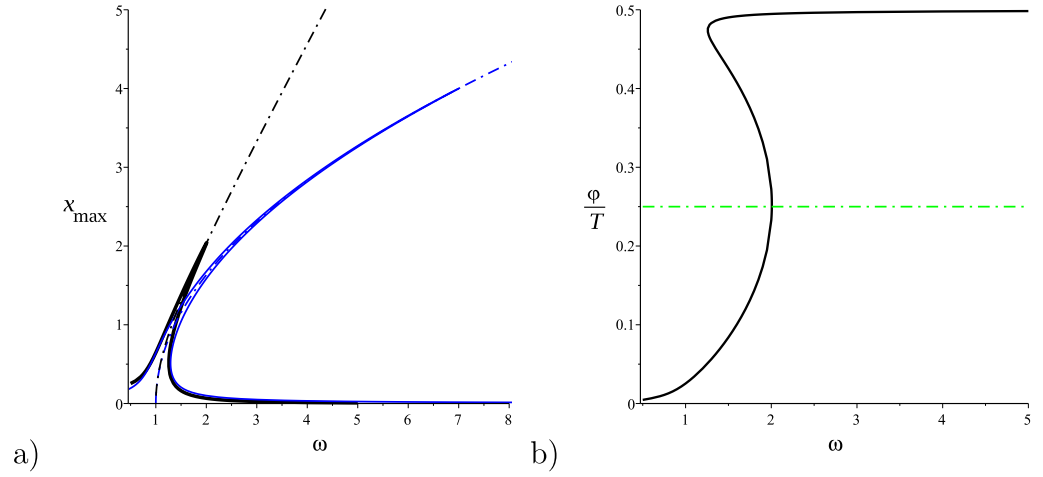

Fig. 3. (a) The backbone (dash–dot) and frequency response (continuous) curves for $\delta = 0.05$ and $F = 0.2$. Blue curves are the asymptotic solutions, and black curves are the exact/numerical ones. (b) The phase difference between the excitation and the solution (only for the numerical solution).

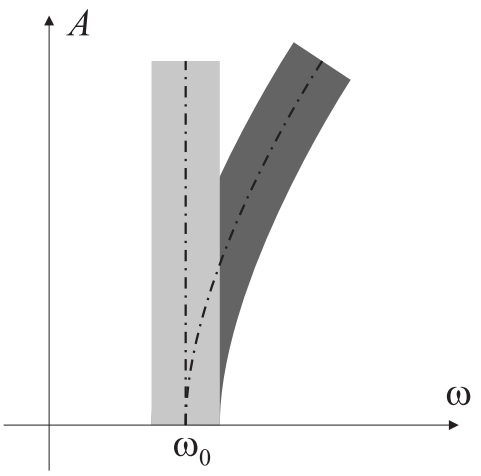

Fig. 4. Schematic representation of the region of validity of classical (light gray strip) and proposed (dark gray strip) asymptotic solutions.

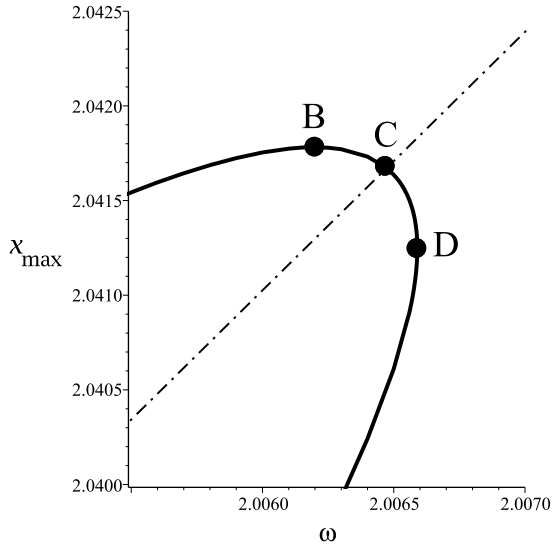

Fig. 5. Enlargement of the numerical FRC around its peak. $\delta = 0.05$ and $F = 0.2$.

Table 1
The coordinates of the three points of Fig. 5.

	ω	x_{max}	φ/T
B	2.0062	2.041781	0.24775
C	2.006468	2.041679	0.25
D	2.006589	2.041245	0.25254

words, organized the development in such a way that the lowest-order term is no longer linear, thus overcoming the limitation (4) of classical methods. This is the approach proposed in this paper, which is illustrated in the following section. Accordingly, it is expected to have accurate results in the dark gray strip of Fig. 4, and thus hopefully the proposed method will give a good approximation of the peak of the FRC also for large values of the excitation amplitudes, where classical methods fail.

2.1. The behavior near the peak

Before proceeding further, it is worth shedding some light on what happens around the peak of the "exact" (i.e. numerical) FRC. An illustrative example is reported in Fig. 5, where we can basically distinguish three relevant points:

(B) The point where the FRC has a maximum in x, i.e. where it has an horizontal tangent;

(C) The point where the FRC intersects the backbone curve;

(D) The point where the FRC has a maximum in ω, i.e. where it has a vertical tangent.

They are very close to each other (see Table 1) and can be undistinguishable from a practical point of view, but remain conceptually distinct. The point B is the most important from a practical point of view since there the displacement is maximum. The point C can be characterized also as the one for which the phase difference is exactly $1/4$ of the period (see Table 1), thus keeping the same property holding for linear systems. The point D corresponds to a Saddle-Node (SN) bifurcation, and there the solution has a jump for increasing ω.

In the classical asymptotic approximation (7) the intersection of the backbone curve and the FRC (i.e. the point C) occurs when the square root is zero (giving $A_{max} = F/\delta$). This point is also the maximum of the amplitude A for varying ω (this can be seen by noting that there $d\omega/dA \to \infty$, so that $dA/d\omega = 0$). In other words, the classical asymptotic method approximates C with B.

3. The proposed asymptotic solution

Let us consider the one-degree-of-freedom system

$$\ddot{x} + f(x) = \varepsilon g(x, \dot{x}, t), \tag{8}$$

where ε is a small parameter and $x(t)$ is the unknown. $f(x)$ is a given, arbitrary *nonlinear* function of x, not requested to be regular although we (implicitly) assume that it is continuous. A problem similar to (8) has been considered in Kovacic (2020), but with a

different solution technique. For the Duffing oscillator, and only with damping terms, the approach has been considered as a "future work" in Morrison (2006), even if to the best of the author's knowledge it has not been further developed and published.

Applying asymptotic methods, the solution is sought after in the form

$$x(t) = x_0(t) + \varepsilon x_1(t) + \varepsilon^2 x_2(t) + \cdots \tag{9}$$

Substituting (9) in (8), and collecting terms multiplying increasing powers of ε we obtain

$$\ddot{x}_0 + f(x_0) = 0, \tag{10}$$

$$\ddot{x}_1 + f'(x_0)x_1 = g(x_0, \dot{x}_0, t), \tag{11}$$

$$\ddot{x}_2 + f'(x_0)x_2 = -\frac{f''(x_0)}{2}x_1^2 + \frac{\partial g(x_0, \dot{x}_0, t)}{\partial x}x_1 + \frac{\partial g(x_0, \dot{x}_0, t)}{\partial \dot{x}}\dot{x}_1, \tag{12}$$

$$\ddot{x}_3 + f'(x_0)x_3 = \cdots$$

It is important to remark that (10), called the "unperturbed equation", is *nonlinear*, and this is the major difference with respect to classical approaches, in which each problem, at any order, is linear. The subsequent equations, on the other hand, are *linear* in their unknowns, but have the non-constant coefficient $f'(x_0)$, contrary to the classical approaches. They can be expressed in the common form

$$\ddot{x}_n + f'(x_0)x_n = h_n(t), \quad n \geq 1, \tag{13}$$

where $h_n(t)$ is a known function (from the previous steps). The homogeneous version of (13) is

$$\ddot{x}_n + f'(x_0)x_n = 0. \tag{14}$$

3.1. Zero-order problem

To obtain the solution to the zero-order problem (10) we observe that it is conservative, and

$$\frac{\dot{x}_0^2}{2} + V(x_0) = c_1 \tag{15}$$

is constant in time. Here

$$V(x_0) = \int_0^{x_0} f(s)ds \tag{16}$$

is the primitive of $f(x_0)$. Note that $V(0) = 0$ by definition.

From (15) one gets

$$\dot{x}_0 = \pm\sqrt{2[c_1 - V(x_0)]}, \tag{17}$$

from which it is possible to draw the orbits in the phase space $(x_0, \dot{x}_0)$. They are symmetric with respect to the axes $\dot{x}_0 = 0$. From (17) it follows

$$dt = \pm\frac{dx_0}{\sqrt{2[c_1 - V(x_0)]}} \tag{18}$$

or, after integrating,

$$t = t(x_0) = c_2 \pm r(x_0), \qquad r(x_0) = \int_0^{x_0} \frac{ds}{\sqrt{2[c_1 - V(s)]}}. \tag{19}$$

Eq. (19)a gives $t(x_0)$. Inverting this function (possibly in a piecewise manner) one gets the general solution $x_0(t)$. It depends on c_1 and c_2, according to the fact that (10) is second-order. They are constant with respect to t, and can be computed for example by the initial conditions. Note that c_2 is the time for which the displacement vanishes, $x_0(c_2) = 0$, which thus corresponds to $V(0) = 0$ and $\dot{x}_0 = \pm\sqrt{2c_1}$. If $V(x_0) \geq 0$, than it corresponds to the maximum of $\dot{x}_0(t)$.

3.2. nth-order problem, $n \geq 1$

To obtain the solution of the nth-order problem (13) we take the derivative of (10) with respect to t:

$$\frac{d^2}{dt^2}\left(\dot{x}_0\right) + f'(x_0)\dot{x}_0 = 0. \tag{20}$$

This proves that

$$y_1 = \dot{x}_0 \tag{21}$$

is one of the two independent solutions of (14). To find the other one we recall that the Wronskian is given by

$$W = y_1\,\dot{y}_2 - \dot{y}_1\,y_2. \tag{22}$$

From the Abel's theorem we have that $\frac{dW}{dt} = 0$, namely $W = c_3$.

Note that (14) is linear and homogeneous, so that the amplitudes of the two independent solutions $y_1(t)$ and $y_2(t)$ are arbitrary. Thus, without loss of generality we can assume $c_3 = 1$. Then

$$y_1\,\dot{y}_2 - \dot{y}_1\,y_2 = 1, \tag{23}$$

which yields the second solution of (14)

$$y_2(t) = y_1(t)\int \frac{dt}{y_1^2(t)}. \tag{24}$$

If $y_1(t) = a_1(t-\hat{t})^\alpha + \cdots$, in a neighborhood of a certain $\hat{t}$, then $y_2(t) = \frac{(t-\hat{t})^{1-\alpha}}{a_1(1-2\alpha)} + \cdots$, so that $y_2(\hat{t})$ vanishes for $\alpha < 1$ and goes to infinity for $\alpha > 1$. The intermediate case $\alpha = 1$, which indeed is the most common, gives $y_2(t) = -\frac{1}{a_1} + \cdots$, and thus $y_2(\hat{t})$ is bounded.

The particular solution of (13) can then be obtained by the method of variation of constants, which gives

$$x_{n,p}(t) = -y_1(t)\int_{t_0}^{t} h_n(s)\,y_2(s)ds + y_2(t)\int_{t_0}^{t} h_n(s)\,y_1(s)ds, \tag{25}$$

where t_0 can be chosen arbitrarily. Thus, the general solution is

$$x_n(t) = c_{5,n}y_1(t) + c_{6,n}y_2(t) + x_{n,p}(t). \tag{26}$$

By using the definition (24) of $y_2(t)$ in the expression (25) we have that, after some computations, a particular solution can be rewritten as

$$x_{n,p}(t) = y_1(t)\int_{t_0}^{t} \frac{I_n(s,s_0)}{y_1^2(s)}ds, \qquad I_n(s,s_0) = \int_{s_0}^{s} h_n(\xi)y_1(\xi)d\xi, \tag{27}$$

where also s_0 can be chosen arbitrarily. As expected, $x_{n,p}(t)$ does *not* depend on the (free) amplitude of $y_1(t)$. For points where $y_1(\hat{t}) = 0$, the same considerations previously done for $y_2(\hat{t})$ are valid.

The general solution then becomes

$$x_n(t) = y_1(t)\left\{c_{5,n} + c_{6,n}\int_{t_0}^{t}\frac{ds}{y_1^2(s)} + \int_{t_0}^{t}\frac{I_n(s,s_0)}{y_1^2(s)}ds\right\}, \tag{28}$$

or, remembering that $y_1(t) = \dot{x}_0(t)$:

$$x_n(t) = \dot{x}_0(t)\left\{c_{5,n} + c_{6,n}\int_{t_0}^{t}\frac{ds}{\dot{x}_0^2(s)} + \int_{t_0}^{t}\frac{I_n(s,s_0)}{\dot{x}_0^2(s)}ds\right\}. \tag{29}$$

The solutions $x_n(t)$ are then fully determined, to any order. The constants $c_{5,n}$ and $c_{6,n}$ can be computed, for example, by the initial conditions (including those required to have periodic solutions).

3.3. Periodic solutions

The case of periodic solution is the most common and of principal interest in this work.

To the zero-order we have a periodic solution with minimum $x_{0,\min}$ and maximum $x_{0,\max}$ when

$$V(x_{0,\min}) = c_1, \quad V(x_{0,\max}) = c_1, \quad V(x) < c_1 \text{ for } x_{0,\min} < x < x_{0,\max}; \tag{30}$$

in other words, $x_{0,\min}$ and $x_{0,\max}$ are two *consecutive* solutions of $V(x) = c_1$. Note that c_1 is a measure of the amplitude of the periodic oscillation (up to the zero-order), since both $x_{0,\min}$ and $x_{0,\max}$ depend on c_1 by (30).

From (18) the period is

$$T = 2[r(x_{0,\max}) - r(x_{0,\min})] = 2\int_{x_{0,\min}}^{x_{0,\max}} \frac{ds}{\sqrt{2[c_1 - V(s)]}}. \tag{31}$$

This expression gives

$$\omega = \frac{2\pi}{T} = \frac{\pi}{r(x_{0,\max}) - r(x_{0,\min})} = \omega(c_1), \tag{32}$$

i.e. how the frequency depends on the (lowest-order) measure of the amplitude c_1, which is the *exact* backbone curve.

Because of the previous hypothesis we have that $x_0(t) = x_0(t+T)$. It follows from (21) that $y_1(t)$ is periodic, too, with the same period. Then, multiplying (13) by $y_1(t)$, integrating from a generic t_0 to $t_0 + T$ and using the periodicity of $y_1(t)$ we obtain

$$\begin{aligned}&[\dot{x}_n(t_0+T) - \dot{x}_n(t_0)]y_1(t_0) - [x_n(t_0+T) - x_n(t_0)]\dot{y}_1(t_0) = \\ &= \int_{t_0}^{t_0+T} h_n(s)y_1(s)ds = I_n(t_0+T, t_0).\end{aligned} \tag{33}$$

It follows that

$$l_n(t_0+T,t_0)=0,\quad \forall t_0, \tag{34}$$

i.e. $l_n(s,.)$ is T-periodic, is a necessary condition for the T-periodicity of $x_n(t_0)$. This is equivalent to the classical solvability condition, and can be discussed in terms of the Fredholm alternative (Fredholm, 1903), although we do not follow this approach and prefer a more direct one.

A corollary of (34) is that $h_n(s)$ must be T-periodic, which agrees with common sense. Note that the (minimal) period of $h_n(s)$ could be an integer fraction of T, so that we can consider also superharmonic resonance. Remembering that $y_1(s)=\dot{x}_0(s)$ and integrating by parts we see that (34) is equivalent to

$$\int_{t_0}^{t_0+T}\dot{h}_n(s)x_0(s)ds=0,\quad \forall t_0. \tag{35}$$

A particular, but interesting, case is when

$$h_1(t)=g(x_0(t),\dot{x}_0(t),t)=-\delta\dot{x}_0(t)+F\cos(\omega t), \tag{36}$$

where δ is the damping coefficient and F and ω are the amplitude and frequency of the periodic excitation, respectively. Eq. (34) then becomes (assuming without loss of generality $t_0=0$)

$$\begin{aligned}
0&=-\delta\int_0^T\dot{x}_0^2(t)dt+F\int_0^T\cos(\omega t)\dot{x}_0(t)dt\\
&=-2\delta\int_{x_{0,\min}}^{x_{0,\max}}\dot{x}_0(x_0)dx_0+2F\int_{x_{0,\min}}^{x_{0,\max}}\cos[\omega\, t(x_0)]dx_0\\
&=-2\delta\int_{x_{0,\min}}^{x_{0,\max}}\sqrt{2[c_1-V(x_0)]}dx_0\\
&+2F\int_{x_{0,\min}}^{x_{0,\max}}\cos\left\{\omega\left[c_2+r(x_0)\right]\right\}dx_0\\
&=-2\delta\int_{x_{0,\min}}^{x_{0,\max}}\sqrt{2[c_1-V(x_0)]}dx_0\\
&+2F\cos(\omega c_2)\int_{x_{0,\min}}^{x_{0,\max}}\cos\left[\omega\, r(x_0)\right]dx_0\\
&-2F\sin(\omega c_2)\int_{x_{0,\min}}^{x_{0,\max}}\sin\left[\omega\, r(x_0)\right]dx_0.
\end{aligned} \tag{37}$$

It can be rewritten as

$$\delta\, b_1=F[\cos(\omega c_2)b_2-\sin(\omega c_2)b_3], \tag{38}$$

where

$$\begin{aligned}
b_1&=\int_{x_{0,\min}}^{x_{0,\max}}\sqrt{2[c_1-V(x_0)]}dx_0>0,\\
b_2&=\int_{x_{0,\min}}^{x_{0,\max}}\cos\left[\omega\, r(x_0)\right]dx_0,\\
b_3&=\int_{x_{0,\min}}^{x_{0,\max}}\sin\left[\omega\, r(x_0)\right]dx_0,
\end{aligned} \tag{39}$$

are coefficients that dependent on c_1.

Eq. (38) can be further rewritten as

$$\frac{\delta}{F}\,m(c_1)=\cos(\omega c_2+\phi), \tag{40}$$

where

$$\cos(\phi)=\frac{b_2}{\sqrt{b_2^2+b_3^2}},\quad \sin(\phi)=\frac{b_3}{\sqrt{b_2^2+b_3^2}},\quad m(c_1)=\frac{b_1}{\sqrt{b_2^2+b_3^2}}>0. \tag{41}$$

When $V(x)$ is symmetric, $V(x)=V(-x)$, that corresponds to an odd function f, $f(x)=-f(-x)$, we have $x_{0,\min}=-x_{0,\max}$ and

$$\begin{aligned}
T&=4\,r(x_{0,\max}),\\
b_1&=2\int_0^{x_{0,\max}}\sqrt{2[c_1-V(x_0)]}dx_0,\\
b_2&=2\int_0^{x_{0,\max}}\cos\left[\omega\, r(x_0)\right]dx_0,
\end{aligned}$$

$$b_3 = 0, \quad \phi = 0, \quad m(c_1) = \frac{b_1}{|b_2|}. \tag{42}$$

Let us fix δ and F. The (periodic) first-order solution can then be obtained as follow:

1. Choose the excitation frequency ω;
2. invert the backbone curve (32) and determine c_1;
3. compute ϕ by (41)a and (41)b, $\phi = \arctan(b_3/b_2)$;
4. compute c_2 by solving (40), which gives the two solutions

$$c_2 = \frac{1}{\omega}\left[\pm\arccos\left(\frac{\delta}{F}\, m(c_1)\right) - \phi\right]; \tag{43}$$

5. at this point the zero-order solution $x_0(t)$ is determined by inverting (19)a;
6. compute the first-order solution $x_1(t)$ by means of (29),

$$x_1(t) = \dot{x}_0(t)\int_{c_2}^{t} \frac{c_{6,1} + l_1(s)}{\dot{x}_0^2(s)}\, ds,$$
$$l_1(s) = \int_{c_2}^{s} [-\delta \dot{x}_0^2(\xi) + F\cos(\omega\xi)\dot{x}_0(\xi)]d\xi, \tag{44}$$

where we have set $t_0 = s_0 = c_2$ and chosen $c_{5,1} = 0$ to guarantee that $x_1(c_2) = 0$, i.e. the same initial condition for $x_0(t)$. The other constant $c_{6,1}$ is selected in such a way that the derivative of $x_1(t)$ is continuous at the points $\hat{t}$ where $\dot{x}_0(\hat{t}) = 0$, i.e. where the integral in (44)a has a singularity. Here the first-order solution has value $x_1(\hat{t}) = -[c_{6,1} + l_1(\hat{t})]/\ddot{x}_0(\hat{t})$ if $\ddot{x}_0(\hat{t}) \neq 0$ (which is the common case).

7. up the first order the solution is $x(t) = x_0(t) + \varepsilon x_1(t)$.

3.4. The behavior near the peak

Since $\cos(\omega c_2 + \phi) \leq 1$ and $m(c_1) > 0$, from (40) it follows that

$$\frac{F}{\delta} \geq m(c_1). \tag{45}$$

This is the "admissibility" condition for the existence of the considered periodic solution. For $F/\delta > m(c_1)$ there are two solutions c_2 (see (43)); for $F/\delta < m(c_1)$ there are no solutions; for $F/\delta = m(c_1)$ there is the unique solution $c_2 = -\phi/\omega$. Thus, $m(c_1)$ is the minimum value of F/δ giving the oscillation with the considered frequency. It identifies, in an *exact* manner, the intersection of the backbone curve with the FRC, i.e. the point "C" in Fig. 5, that is poorly detected by classical asymptotic methods, as we have shown in Section 2 (see Figs. 2 and 3). Consequently, it also gives a physical meaning to the function $m(c_1)$. The frequency corresponding to this point is

$$\omega(c_1) = \omega[m^{-1}(F/\delta)]. \tag{46}$$

It is worth stressing that we obtained this fundamental information without solving explicitly the various order problems, not even the lowest one, and without special tricks like multiple time scales: just computing the integrals in (39). Thus, it is very simple and powerful.

Let us reconsider the inequality (45) from a different point of view, by assuming that F/δ is fixed. Let $c_{1,cr}$ be the value of c_1 such that $F/\delta = m(c_{1,cr})$. If $m(c_1)$ is monotonically increasing, for $c_1 > c_{1,cr}$ we have $m(c_1) > m(c_{1,cr}) = F/\delta$ and so there are no solutions; clearly, for $c_1 < c_{1,cr}$ there are two solutions. If $\omega(c_1)$ is monotonically increasing (i.e. we have a hardening behavior), for $\omega(c_1) > \omega(c_{1,cr}) = \omega_{cr}$ we have $c_1 > c_{1,cr}$ and so there are no solutions; for $\omega(c_1) < \omega_{cr}$ there are two solutions. Thus at ω_{cr} there is a SN bifurcation.

The same conclusion can be obtained if $m(c_1)$ and/or $\omega(c_1)$ are monotonically decreasing, possibly changing the side where there are two solutions (i.e. for $\omega > \omega_{cr}$ instead of $\omega < \omega_{cr}$), but still keeping the SN bifurcation (possibly of reverse type).

The previous results show that the proposed approach approximates point C with point D of Fig. 5, and this marks a conceptual difference with respect to the classical asymptotic methods (see the last sentence of Section 2). From a practical point of view, however, all three points of Fig. 5 coincide, and so we "exactly" compute also the point B, for any value of F and δ, which is the big advance of the proposed method.

From (19) we have that the time $t_{\max}$ in correspondence of the maximum value $x_{0,\max}$ is

$$t_{\max} = c_2 + r(x_{0,\max}). \tag{47}$$

In the case of symmetric $V(x)$ we have $\phi = 0$, so that $c_2 = 0$, and $x_{0,\min} = -x_{0,\max}$. Comparing then (47) with (42)a we conclude that $t_{\max} = T/4$. Since the excitation $\cos(\omega t)$ has a maximum in $t = 0$ we note that the phase difference between the excitation and the solution is $T/4$, in perfect agreement with the findings of Section 2.1.

4. Examples

4.1. The linear equation

To start with a simple example, and to check that our developments are ground on solid foundations, we initially consider the linear case, i.e.

$$f(x) = x, \quad V(x) = \frac{x^2}{2}, \quad g(x,\dot{x},t) = -\delta\dot{x} + F\cos(\omega t). \tag{48}$$

We have

$$r(x_0) = \arcsin\left(\frac{x_0}{x_{0,\max}}\right), \quad T = 4\,r(x_{0,\max}) = 2\pi,$$
$$b_1 = \frac{x_{0,\max}^2\pi}{2}, \quad b_2 = \frac{x_{0,\max}\pi}{2} \quad \rightarrow \quad m = x_{0,\max}, \tag{49}$$

so that $F/\delta = x_{0,\max}$, which is the exact value of intersection of the FRC with the backbone curve, that in this simple case is frequency independent and given by $\omega = 1$.

4.2. The Duffing equation

A fully nonlinear case is the classical Duffing Eq. (3), i.e.

$$f(x) = x + x^3, \quad V(x) = \frac{x^2}{2} + \frac{x^4}{4}, \quad g(x,\dot{x},t) = -\delta\dot{x} + F\cos(\omega t), \tag{50}$$

which has been considered also in Section 2 because it is a very interesting example of a nonlinear oscillator. Note that it has a symmetric potential.

We have

$$r(x_0) = \int_0^{x_0} \frac{ds}{\sqrt{2[V(A) - V(s)]}} = \sqrt{\frac{2}{2+A^2}}\,F1\left(\frac{x_0}{A}, \frac{IA}{\sqrt{2+A^2}}\right), \tag{51}$$

where $A = x_{0,\max}$, $F1(x)$ is the incomplete elliptic integral of the first kind (Abramowitz & Stegun, 1965; Byrd & Friedman, 1954) and I is the imaginary unit.

Using (51), the period and circular frequency, computed by means of (42)a, are

$$T = 4\sqrt{\frac{2}{2+A^2}}\,K\left(\frac{IA}{\sqrt{2A^2}}\right), \quad \omega = \frac{2\pi}{T}, \tag{52}$$

where $K(x)$ is the complete elliptic integral of the first kind (Byrd & Friedman, 1954).

From (42)b we have that

$$b_1 = \frac{2\sqrt{2}}{3}\sqrt{2+A^2}\left[(1+A^2)K\left(\frac{IA}{\sqrt{2+A^2}}\right) - E\left(\frac{IA}{\sqrt{2+A^2}}\right)\right], \tag{53}$$

where $E(x)$ is the complete elliptic integral of the second kind (Byrd & Friedman, 1954); it is shown in Fig. 6a. The function $b_2(A)$, on the other hand, cannot be computed in closed-form, but can be easily determined numerically, taking advantage of (51); it is reported in Fig. 6b, which shows that it is practically linear.

Once b_1 and b_2 are known, it is immediate to compute m by (42) and ω by (46). Inverting the former we can compute $A(F/\delta)$ and then $\omega(F/\delta)$, which are reported in Fig. 7. They can be used to determined the exact frequency and amplitude of the "peak" of the FRC as a function of F/δ: more precisely, they give the coordinates of the point C of intersection between the FRC and the backbone curve, which is very close to the maximum value of the FRC and to the SN bifurcation point, see Fig. 5. For example, for $F = 0.2$ and $\delta = 0.05$, i.e. $F/\delta = 4$, we have $x_{0,\max} = 2.041679$ and $\omega = 2.0064684$, that perfectly agrees with the coordinates of the point C of Table 1, that there have been computed by numerical simulations. For $F = 0.05$ we have $x_{0,\max} = 0.82571$ and $\omega = 1.22642$ that gives the coordinates of the peak of Fig. 2, while for $F = 0.015$ we have $x_{0,\max} = 0.29160$ and $\omega = 1.03132$ that agree with Fig. 1.

The periodic solution of the zero-order problem is

$$x_0(t) = A\,cn(s,b), \tag{54}$$

where

$$s = a\,t + \beta, \quad a^2 = 1 + A^2, \quad b^2 = \frac{1}{2}\frac{A^2}{A^2+1}, \tag{55}$$

and where A (the amplitude) and β (the phase) are to be determined. It follows that

$$y_1 = \dot{x}_0 = -A\,a\,sn(s,b)dn(s,b),$$
$$y_2 = \frac{1}{A\,a^2}\left\{dn(s,b)\,sn(s,b)\,E[sn(s,b),b]\frac{2b^2-1}{b^2-1}\right.$$

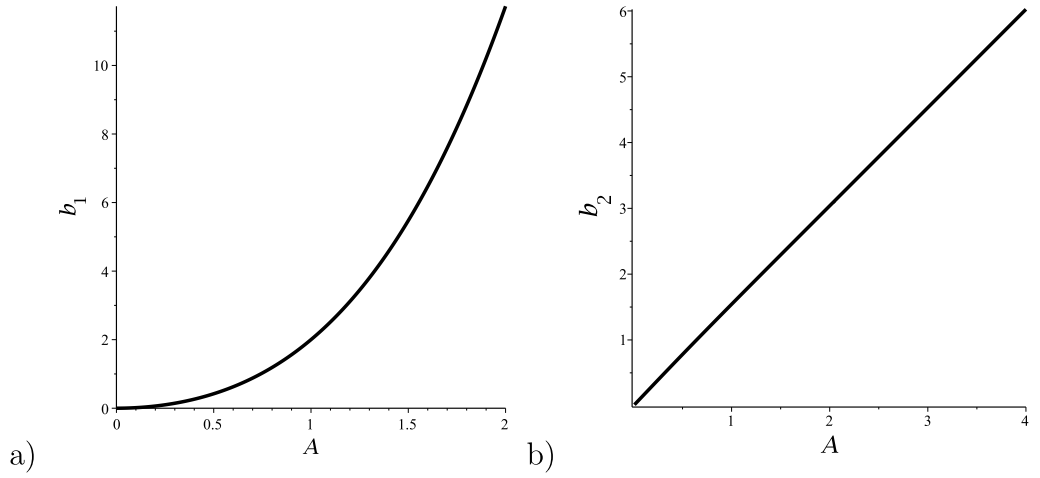

Fig. 6. The functions (a) $b_1(A)$ and (b) $b_2(A)$.

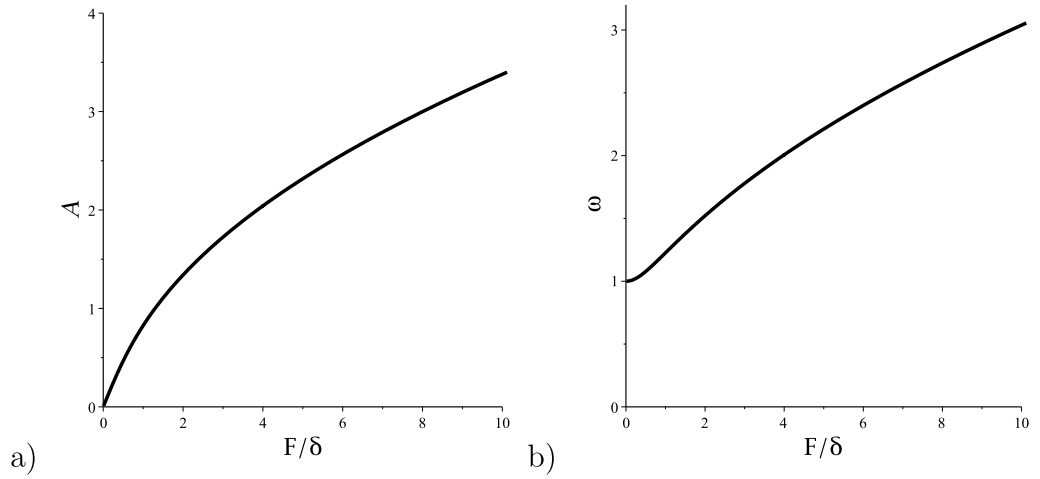

Fig. 7. The functions (a) $A(F/\delta)$ and (b) $\omega(F/\delta)$. They give the coordinates of the peak of the FRC as a function of F/δ.

$$- \, sn^2(s,b)\, dn(s,b)\, cn(s,b) \left[\frac{b^4}{(b^2-1)dn(s,b)} + \frac{dn(s,b)\, b^2}{dn^2(s,b)-1} \right]$$
$$-s\, dn\,(s,b)\, sn\,(s,b)\} \,. \tag{56}$$

Note that y_2 is unbounded (see the last term, proportional to s). cn, sn and dn are the Jacobian elliptic functions (Abramowitz & Stegun, 1965; Byrd & Friedman, 1954), and E is the complete elliptic integral of the second type.

The first-order solution is computed by means of (44). As an illustrative case we consider $F = 0.2$, $\delta = 0.05$ and $\omega = 1.4$ ($T = 4.48799$), which is in between the linear frequency $\omega_0 = 1$ and the peak frequency $\omega_{peak} = 2.0064684$ computed above.

From (43) we have that the two solutions are $c_{2,\pm} = \pm 0.8333$ (note that $c_2 \neq 0$ because we are not on the peak of the FRC); then β is determined in such a way that $x_0(c_{2\pm}) = 0$, which gives $\beta_\pm = -a(T/4 + c_{2\pm})$, namely $\beta_+ = -2.96997$ and $\beta_- = -0.43851$. This is enough to determine the two functions $l_{1\pm}(t)$, that are reported in Fig. 8.

Next we observe that $\dot{x}_0$ vanishes for $\hat{t} = c_{2\pm} + T/4$. Imposing the continuity of $\dot{x}_1(t)$ at $\hat{t}$ we obtain $c_{6,1\pm} = \mp 0.2334$. With this we are able to determine $x_{1\pm}(t)$, that are reported in Fig. 9.

Summing $x_0(t)$ and $x_1(t)$ we are finally able to determine the two solutions $x_\pm(t)$ up to the first order. They are depicted in red in Fig. 10, where they are compared with the corresponding numerical ones (in black) obtained in Section 2. A noticeable agreement is observed, which confirms the validity of the proposed approach for large values of the oscillation amplitude.

The closeness of the analytical and numerical solutions is confirmed also from a quantitative point of view, since for the upper solution we have $x_{\max} = 1.27535$ (analytical) vs $x_{\max} = 1.23210$ (numerical) and the phase differences between the excitation and the oscillation are $\varphi/T = 0.064326$ (analytical) vs $\varphi/T = 0.069334$ (numerical). For the lower solution, we have $x_{\max} = 1.01128$ (analytical) vs $x_{\max} = 1.02455$ (numerical) and $\varphi/T = 0.43567$ (analytical) vs $\varphi/T = 0.44240$ (numerical).

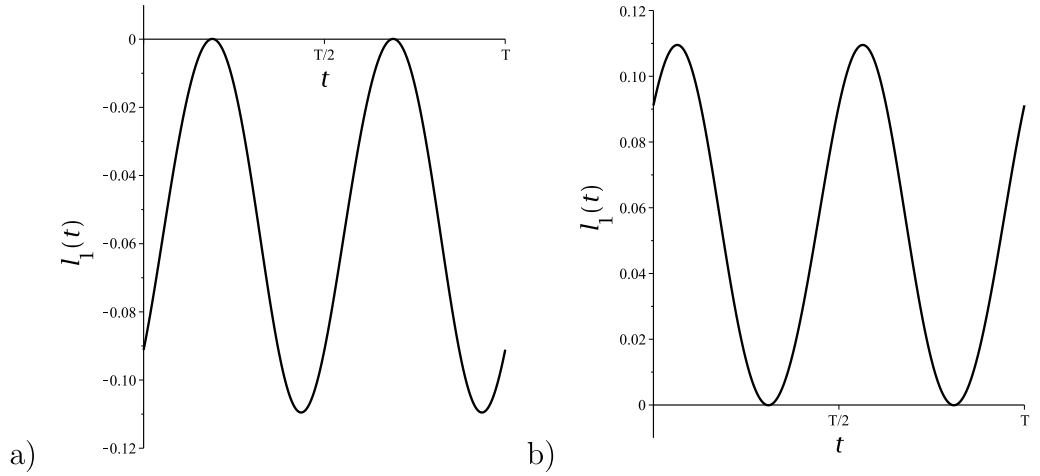

Fig. 8. The functions (a) $l_{1+}(t)$ and (b) $l_{1-}(t)$. $\delta = 0.05$, $F = 0.2$ and $\omega = 1.4$.

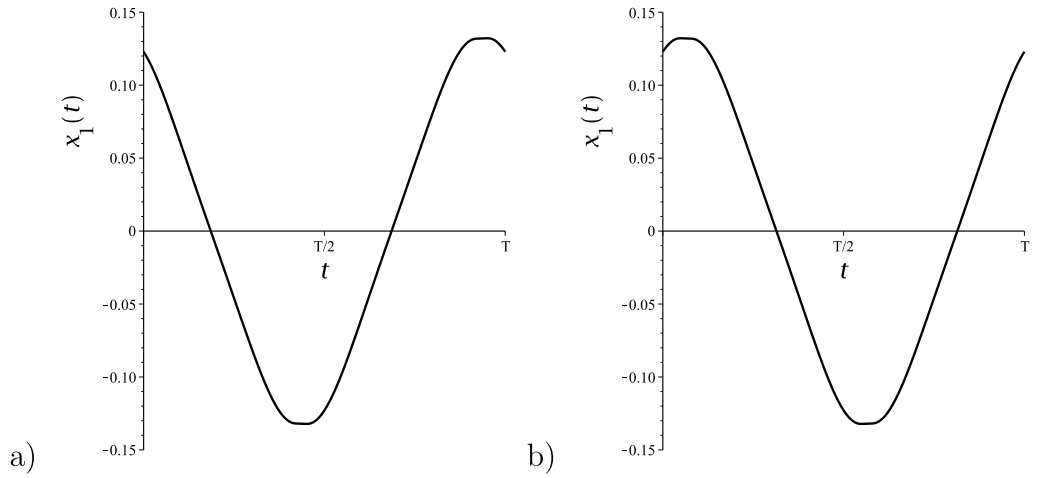

Fig. 9. The functions (a) $x_{1+}(t)$ and (b) $x_{1-}(t)$. $\delta = 0.05$, $F = 0.2$ and $\omega = 1.4$.

Repeating the same computation illustrated above for different values of ω (but keeping fixed F and δ) we can determine the FRC, which is reported in red in Fig. 11a, where it is compared with the corresponding numerical one (in black), computed in Section 2. The agreement is excellent around the peak and decreases only for lower values of the excitation frequency, where the FRC moves far away from the backbone curve. This is in perfect agreement with the considerations related to Fig. 4. The agreement between analytical and numerical solutions is also excellent in terms of the phase difference, as illustrated in Fig. 11b.

By comparing Figs. 3 and 11 it is evident the superior performances of the proposed method with respect to the classical asymptotic developments.

To end this subsection it is worth to report in Fig. 12 two enlargements of Fig. 11a. Fig. 12a further proves the closeness of theoretical and numerical results, even to an enlarged scale, while Fig. 12b illustrates what is said in Section 2.1, i.e. that the proposed approach approximates point C with point D of Fig. 5. Looking at the axes scales, it is further confirmed that this difference has only a theoretical meaning, and is negligible from a practical point of view.

4.3. The Helmholtz equation

In the previous section we have investigated the simplest case of symmetrical hardening nonlinear oscillator. To deal with a non-symmetrical and softening example, in this section we consider the Helmholtz oscillator, i.e.

$$f(x) = x + x^2, \quad V(x) = \frac{x^2}{2} + \frac{x^3}{3}, \quad g(x, \dot{x}, t) = -\delta\dot{x} + F\cos(\omega t). \tag{57}$$

Bounded oscillations exist for $V < 1/6$, in the interval $-1 < x < 1/2$.

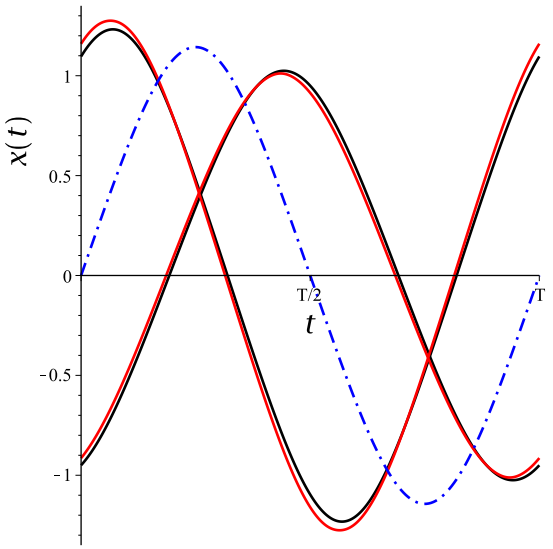

Fig. 10. The functions $x_{\pm}(t)$. In red the analytical solution up to the first, in black the numerical solution. The dash–dot blue curve is the free oscillation of the system for the same value of ω. $\delta = 0.05$, $F = 0.2$ and $\omega = 1.4$.

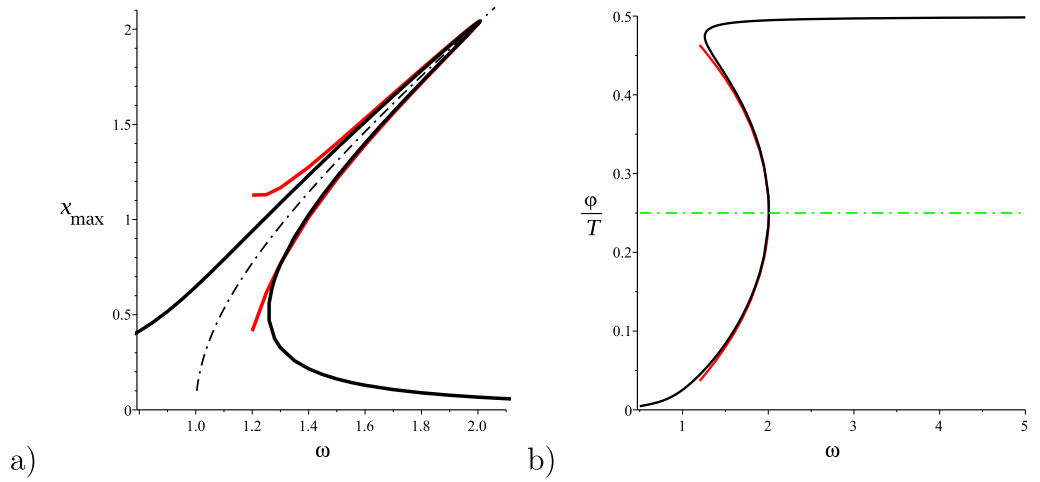

Fig. 11. (a) Analytical (red) and numerical (black) FRCs. (b) Analytical (red) and numerical (black) phase difference between the excitation and the solution. $\delta = 0.05$ and $F = 0.2$.

Similarly to the Duffing case, also here the function $r(x_0)$ can be computed in terms of the incomplete elliptic integral of the first kind:

$$r(x_0) = \int_0^{x_0} \frac{ds}{\sqrt{2[V(A) - V(s)]}} = \sqrt{\frac{-24}{3 + 6A + \bar{A}}} \times$$
$$\times \left[F1\left(\sqrt{\frac{1}{2} + \sqrt{\frac{1}{12}\frac{3+2A}{1-2A}} + \frac{2x_0}{\bar{A}}}, \sqrt{\frac{2}{1 + 3\frac{1+2A}{\bar{A}}}} \right) - \right.$$
$$\left. - F1\left(\sqrt{\frac{1}{2} + \sqrt{\frac{1}{12}\frac{3+2A}{1-2A}}}, \sqrt{\frac{2}{1 + 3\frac{1+2A}{\bar{A}}}} \right) \right],$$
$$\bar{A} = \sqrt{3(3 + 2A)(1 - 2A)}. \tag{58}$$

Using (58) it is possible to compute the backbone curve, which is reported in Fig. 13, where both the maximum and the minimum values of the displacements (that are not longer equal in absolute value) are illustrated. The softening behavior is clear, and it is

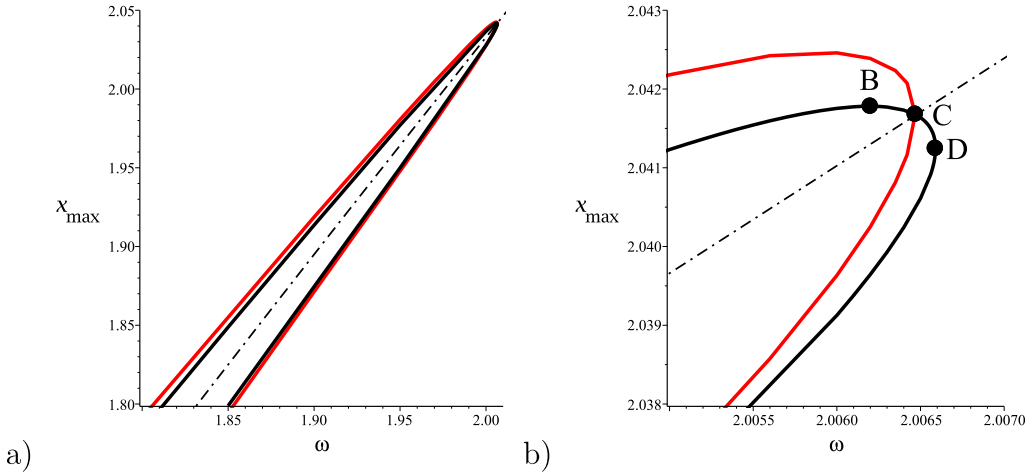

Fig. 12. Enlargements of Fig. 11a.

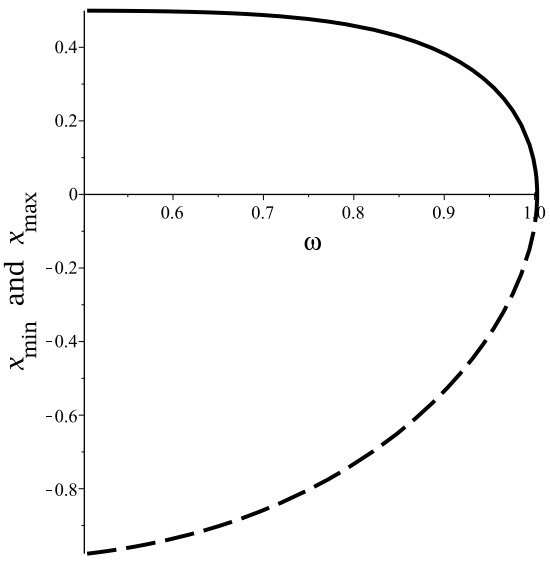

Fig. 13. The backbone curves for the Helmholtz oscillator.

noted that $x_{max} \to 1/2$ and $x_{min} \to -1$ for $\omega \to 0$. In this limit case, the periodic solution tends to the homoclinic solution of the hilltop saddle at $x = -1$.

The functions $x_{max}(F/\delta)$, $x_{min}(F/\delta)$ and $\omega(F/\delta)$, giving the coordinates of the peak of the FRC, are illustrated in Figs. 14a and 14b, to be compared with Fig. 7 to ascertain the effect of asymmetry and softening. In Fig. 14c it is reported the function $\phi(F/\delta)$ (see (41)), which is no longer null since the potential is not symmetric. An important property is that all functions turn back at about $F/\delta = 0.509$, thus showing a very peculiar behavior of this system.

4.4. The quintic equation

As a final example we consider the quintic equation

$$f(x) = x + x^3 - x^5, \quad V(x) = \frac{x^2}{2} + \frac{x^4}{4} - \frac{x^6}{6},$$
$$g(x, \dot{x}, t) = -\delta\dot{x} + F\cos(\omega t), \tag{59}$$

which is symmetric but with a *non* monotonic backbone curve, which is reported in Fig. 15.

The solution is reported in Fig. 16, where it is confirmed the non-monotonic behavior for large values of F/δ already observed for the Helmholtz oscillator. Thus, we guess that it is due to the softening behavior shared by these two systems.

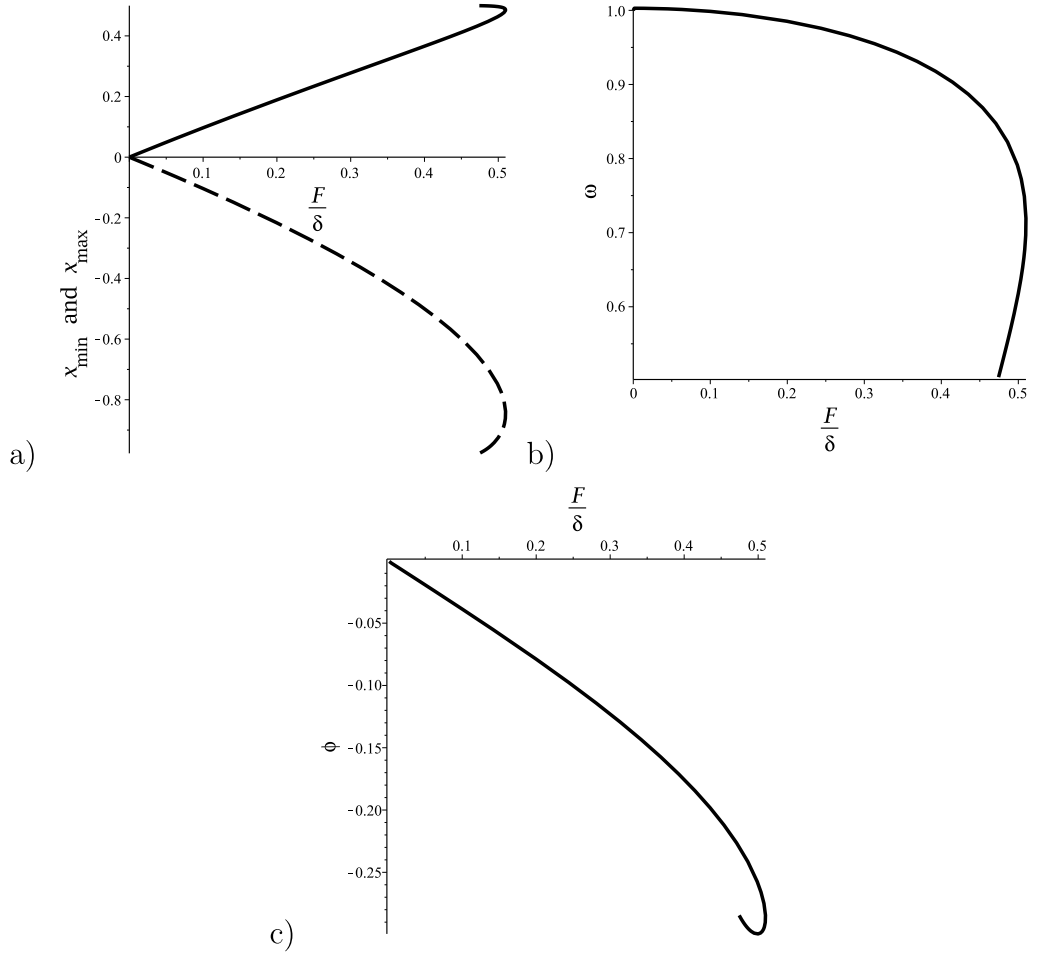

Fig. 14. The functions (a) $x_{\max}(F/\delta)$ and $x_{\min}(F/\delta)$ and (b) $\omega(F/\delta)$. They give the coordinates of the peak of the FRC as a function of F/δ. (c) The function $\phi(F/\delta)$. Helmholtz oscillator.

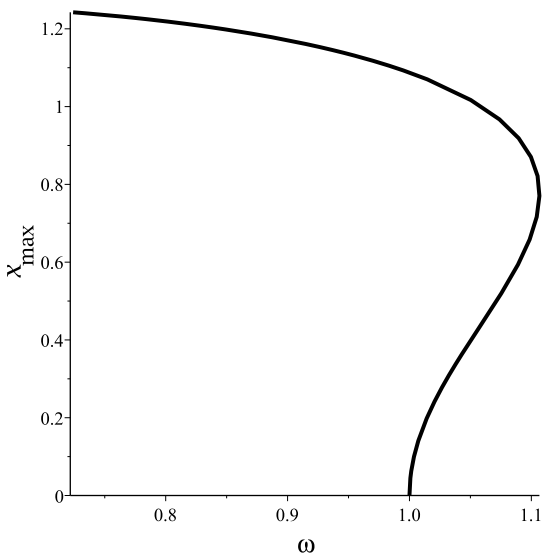

Fig. 15. The backbone curve for the quintic oscillator.

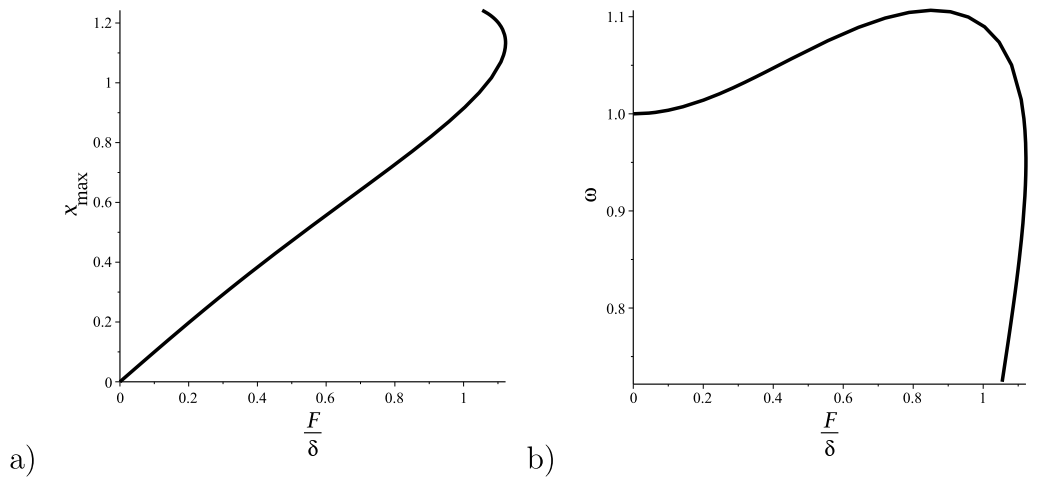

Fig. 16. The functions (a) $x_{max}(F/\delta)$ and (b) $\omega(F/\delta)$. They give the coordinates of the peak of the FRC as a function of F/δ. Quintic oscillator.

5. Conclusions and further developments

A novel asymptotic method for detecting analytically the nonlinear oscillations of generic systems is proposed. The basic idea consists of having the zero-order problem, the dominating one, that is nonlinear, thus extending the classical approaches where the lowest-order problem is linear.

Taking advantage of the conservativeness of the zero-order problem, the solution is obtained analytically. Also, the exact solution is obtained for higher-order problems, thus providing a fully analytical approach. This is obtained for a completely generic system, and thus the approach is not restricted to specific cases or to specific solutions.

Attention is then focused on periodic oscillations, and it is shown how the proposed method allows us to compute exactly the peak of the frequency response curves, by means of simple integrals and without complicated tricks like in the multiple time scale method.

The performances of the proposed method are illustrated with reference to the classical Duffing oscillator, which also has an interest *per se*. The near peak behavior is initially illustrated with numerical simulations, showing some properties that, to the best of the author's knowledge, have not been highlighted before. Then, the analytical solution is computed, and compared with the numerical one, showing an excellent agreement in the top part of the frequency response curve, where classical approaches commonly fail.

The method has been applied also to other simple oscillators, to show how it works for non-symmetrical and softening behavior, as well as for non-monotonic FRCs.

The most important further development consists of dealing with the stability of the proposed oscillations. Also considering different excitations (e.g. parametric) and different dampings (e.g. quadratic), which can be easily addressed with the proposed method, are worthy of further investigations. Different mechanical systems, possibly non-smooth, needs successive study, too. We finally mention the extension to higher dimensional systems (including continuous systems, that may also have the boundary layer problem and thus joining asymptotic methods in time and space), although it is foreseen that some mathematical difficulties may arise due to the dimension. In this respect, help can come from the nonlinear normal mode theory, which could simplify the computations of the backbone curve, together with the Rauscher method, along the lines developed for example in Section 5 of Vakakis, Manevitch, Mikhlin, Pilipchuk, and Zevin (1996).

Declaration of competing interest

The authors declare that they have no known competing financial interests or personal relationships that could have appeared to influence the work reported in this paper.

Data availability

No data was used for the research described in the article.

Acknowledgment

This work has been partially written within the belonging of SL to the Gruppo Nazionale di Fisica Matematica (GNFM). The author wishes to thank Prof. Yuri Mikhlin and Prof. Angelo Luongo for useful discussions related to the topic of this paper. The paper has been partially developed within the "DICEA Dipartimento di Eccellenza 2023" project, funded by the Italian MUR.

References

Abramowitz, M., & Stegun, I. A. (Eds.), (1965). *Handbook of mathematical functions*. Dover, ISBN: 0-486-61272-4.

Alfosail, F. K., & Younis, M. I. (2020). Multifrequency excitation of an inclined marine riser under internal resonances. *Nonlinear Dynamics*, *99*, 149–171. http://dx.doi.org/10.1007/s11071-019-05136-w.

Atluri, S. (1973). Nonlinear vibrations of hinged beam including nonlinear inertia effects. *ASME Journal of Applied Mechanics*, *40*, 121–126. http://dx.doi.org/10.1115/1.3422909.

Awrejcewicz, J., Andrianov, I. V., & Manevitch, L. I. (1998). *Asymptotic approaches in nonlinear dynamics*. Berlin: Springer, ISBN: 3-540-63894-6.

Awrejcewicz, J., & Krysko, V. A. (2006). *Introduction to asymptotic methods*. Boca Raton: Chapman & Hall, ISBN: 1-58488-677-3.

Bauomy, H., & Taha, A. (2021). Nonlinear saturation controller simulation for reducing the high vibrations of a dynamical system. *Mathematical Biosciences and Engineering*, *19*, 3487–3508. http://dx.doi.org/10.3934/mbe.2022161.

Belhaq, M., & Lakrad, F. (2000). The elliptic multiple scales method for a class of autonomous strongly non-linear oscillators. *Journal of Sound and Vibration*, *234*, 547–553. http://dx.doi.org/10.1006/jsvi.2000.2883.

Bensoussan, A., Lions, J. L., & Papanicolaou, G. (2011). *Asymptotic analysis for periodic structures*. American Mathematical Society: Rhode Island, ISBN: 978-0-8218-5324-5.

Bogoliubov, N. N., & A., Mitropolskii Yu. (1961). *Asymptotic methods in the theory of nonlinear oscillations*. New York: Gordon and Breach, ISBN: 0-677-20050-1.

Brasil, R. M. L. R. F. (1999). Multiple scales analysis of nonlinear oscillations of a portal frame foundation for several machines. *Journal of the Brazilian Society of Mechanical Sciences*, *21*, 641–654. http://dx.doi.org/10.1590/S0100-73861999000400007.

Brennan, M. J., & Kovacic, I. (Eds.), (2011). *Duffing's equation: Non-linear oscillators and their behavior*. John Wiley & Sons, ISBN: 978-0-470-71549-9.

Byrd, P., & Friedman, M. (1954). *Handbook of elliptic integrals for engineers and physicists*. Berlin: Springer-Verlag, ISBN: 978-3-642-65138-0.

Cartmell, M. P., Ziegler, S. W., Khanin, R., & Forehand, D. I. M. (2003). Multiple scales analyses of the dynamics of weakly nonlinear mechanical systems. *Applied Mechanics Review*, *56*, 455–492. http://dx.doi.org/10.1115/1.1581884.

Chen, S. H., & Cheung, Y. K. (1997). An elliptic Lindstedt–Poincaré method for certain strongly non-linear oscillators. *Nonlinear Dynamics*, *12*, 199–213. http://dx.doi.org/10.1023/A:1008267817248.

Clementi, F., Lenci, S., & Rega, G. (2020). 1:1 Internal resonance in a two d.o.f. complete system: a comprehensive analysis and its possible exploitation for design. *Meccanica*, *55*, 1309–1332. http://dx.doi.org/10.1007/s11012-020-01171-9.

Duffing, G. (1918). *Forced oscillators with variable eigenfrequency and their technical meaning* (pp. 41–42). Sammlung Vieweg: Vieweg & Sohn (in German).

Elias-Zuniga, A. (2005). Application of Jacobian elliptic functions to the analysis of the steady-state solution of the damped Duffing equation with driving force of elliptic type. *Nonlinear Dynamics*, *42*, 175–184. http://dx.doi.org/10.1007/s11071-005-2554-0.

Elias-Zuniga, A. (2006). A general solution of the Duffing equation. *Nonlinear Dynamics*, *45*, 227–235. http://dx.doi.org/10.1007/s11071-006-1858-z.

Fortunati, A., Bacigalupo, A., Lepidi, M., Arena, A., & Lacarbonara, W. (2022). Nonlinear wave propagation in locally dissipative metamaterials via Hamiltonian perturbation approach. *Nonlinear Dynamics*, *108*, 765–787. http://dx.doi.org/10.1007/s11071-022-07199-8.

Fredholm, E. I. (1903). Sur une classe d'equations fonctionnelles. *Acta Mathematica*, *27*, 365–390. http://dx.doi.org/10.1007/BF02421317.

Gonçalves, P. B., Silva, F. M. A., & Del Prado, Z. J. G. N. (2008). Low-dimensional models for the nonlinear vibration analysis of cylindrical shells based on a perturbation procedure and proper orthogonal decomposition. *Journal of Sound and Vibration*, *315*, 641–663. http://dx.doi.org/10.1016/j.jsv.2008.01.063.

Guo, T., Rega, G., Kang, H., & Wang, L. (2020). Two perturbation formulations of the nonlinear dynamics of a cable excited by a boundary motion. *Applied Mathematical Modelling*, *79*, 434–450. http://dx.doi.org/10.1016/j.apm.2019.10.045.

Hinch, E. J. (1991). *Perturbation methods*. Cambridge: Cambridge University Press, ISBN: 0-521-37897-4.

Holmes, M. H. (1995). *Introduction to perturbation methods*. New York: Springer-Verla, ISBN: 0-387-94203-3.

Hsu, C. S. (1960). On the application of elliptic functions in nonlinear forced oscillations. *Quarterly of Applied Mathematics*, *17*, 393–407.

Ilyas, S., Alfosail, F. K., & Younis, M. I. (2019). On the application of the multiple scales method on electrostatically actuated resonators. *Journal of Computational and Nonlinear Dynamics*, *14*, Article 041006. http://dx.doi.org/10.1115/1.4042694.

Kevorkian, J., & Cole, J. D. (1981). *Applied mathematical sciences: vol. 34, Perturbation methods in applied mathematics*. New York: Springer-Verlag, ISBN: 978-1-4419-2812-2.

Kloda, L., Lenci, S., & Warminski, J. (2018). Nonlinear dynamics of a planar beam-spring system: analytical and numerical approaches. *Nonlinear Dynamics*, *94*, 1721–1738. http://dx.doi.org/10.1007/s11071-018-4452-2.

Kloda, L., Lenci, S., Warminski, J., & Szmit, Z. (2022). Flexural-flexural internal resonances 3:1 in initially straight, extensible timoshenko beams with an axial spring. *Journal of Sound and Vibration*, *527*, Article 116809-1-18. http://dx.doi.org/10.1016/j.jsv.2022.116809.

Kovacic, I. (2020). *Nonlinear oscillations. Exact solutions and their approximation*. Springer, ISBN: 978-3-030-53171-3.

Kovacic, I., Cveticanin, L., Zukovic, M., & Rakaric, Z. (2016). Jacobi elliptic functions: A review of nonlinear oscillatory application problems. *Journal of Sound and Vibration*, *380*, 1–36. http://dx.doi.org/10.1016/j.jsv.2016.05.051.

Lenci, S., Clementi, F., & Mazzilli, C. E. N. (2013). Simple formulas for the natural frequencies of non-uniform cables and beams. *International Journal of Mechanical Sciences*, *77*, 155–163. http://dx.doi.org/10.1016/j.ijmecsci.2013.09.028.

Li, L., & Hu, Y. (2016). Nonlinear bending and free vibration analyses of nonlocal strain gradient beams made of functionally graded material. *International Journal of Engineering Science*, *107*, 77–97. http://dx.doi.org/10.1016/j.ijengsci.2016.07.011.

Luongo, A. (2017). On the use of the multiple scale method in solving 'difficult' bifurcation problems. *Mathematics and Mechanics of Solids*, *22*, 988–1004. http://dx.doi.org/10.1177/1081286515616053.

Luongo, A., & Zulli, D. (2012). Dynamic analysis of externally excited NES-controlled systems via a mixed Multiple Scale/Harmonic Balance algorithm. *Nonlinear Dynamics*, *70*, 2049–2061. http://dx.doi.org/10.1007/s11071-012-0597-6.

Luongo, A., Zulli, D., & Piccardo, G. (2008). Analytical and numerical approaches to nonlinear galloping of internally resonant suspended cables. *Journal of Sound and Vibration*, *315*, 375–393. http://dx.doi.org/10.1016/j.jsv.2008.03.067.

Morrison, T. M. (2006). *Three problems in nonlinear dynamics with 2:1 parametric excitation* (Ph.D. thesis), Cornell University.

Nayfeh, A. (1973). *Perturbation methods*. New York: Wiley-Interscience, ISBN: 0-471-63059-4.

Nayfeh, A. (1993). *Introduction to perturbation techniques*. New York: Wiley-Interscience, ISBN: 0-471-31013-1.

Nayfeh, A. H., & Mook, D. (1995). *Nonlinear oscillations*. New York: Wiley, ISBN: 0-471-12142-8.

Nie, J. F., Zheng, M. L., Yu, G. B., Wen, J. M., & Dai, B. (2013). The method of multiple scales in solving nonlinear dynamic differential equations of gear systems. *Applied Mechanics and Materials*, *274*, 324–327. http://dx.doi.org/10.4028/www.scientific.net/amm.274.324.

Parzygnat, W. J., & Pao, Y.-H. (1978). Resonance phenomena in the nonlinear vibration of plates governed by Duffing's equation. *International Journal of Engineering Science*, *16*, 999–1017. http://dx.doi.org/10.1016/0020-7225(78)90057-5.

Rand, R. H., & Armbruster, D. (1987). *Applied mathematical sciences: vol. 59, Perturbation methods, bifurcation theory and computer algebra*. New York: Springer-Verlag, ISBN: 978-1-4612-1060-3.

Razzak, M. A., Alam, M. Z., & Sharif, M. N. (2018). Modified multiple time scale method for solving strongly nonlinear damped forced vibration systems. *Results in Physics*, *8*, 231–238. http://dx.doi.org/10.1016/j.rinp.2017.12.015.

Ren, Z.-F., Yao, S.-W., & He, J.-H. (2019). He's multiple scales method for nonlinear vibrations. *Journal of Low Frequency Noise, Vibration and Active Control*, *38*, 1708–1712. http://dx.doi.org/10.1177/1461348419861450.

Settimi, V., Gottlieb, O., & Rega, G. (2015). Asymptotic analysis of a noncontact AFM microcantilever sensor with external feedback control. *Nonlinear Dynamics*, *79*, 2675–2698. http://dx.doi.org/10.1007/s11071-014-1840-0.

Srinil, N., & Rega, G. (2007). The effects of kinematic condensation on internally resonant forced vibrations of shallow horizontal cables. *International Journal of Non-Linear Mechanics*, *42*, 180–195. http://dx.doi.org/10.1016/j.ijnonlinmec.2006.09.005.

Vakakis, A. F., Manevitch, L. I., Mikhlin, Y. V., Pilipchuk, V. N., & Zevin, A. A. 1996. John Wiley & sons, ISBN: 0-471-13319-1.

Xu, X., & Wiercigroch, M. (2007). Approximate analytical solutions for oscillatory and rotational motion of a parametric pendulum. *Nonlinear Dynamics*, *47*, 311–320. http://dx.doi.org/10.1007/s11071-006-9074-4.

Yang, Z., Sun, Y., Liu, Y., & Cui, J. (2021). Prediction on nonlinear mechanical performance of random particulate composites by a statistical second-order reduced multiscale approach. *Acta Mechanica Sinica*, *37*, 570–588. http://dx.doi.org/10.1007/s10409-020-01025-3.